Oligotyping and Genome-Resolved Metagenomics Reveal Distinct *Candidatus* Accumulibacter Communities in Full-Scale Side-Stream versus Conventional Enhanced Biological Phosphorus Removal (EBPR) Configurations

Running Title: Oligotyping reveals clade differences of Accumulibacter

Varun N. Srinivasan[1], Guangyu Li[1], Dongqi Wang[1,2], Nicholas B. Tooker[1,3], Zihan Dai[4], Annalisa Onnis-Hayden[1], Ameet Pinto[1], April Z. Gu[1,5*]

[1]Department of Civil and Environmental Engineering, Northeastern University, Boston MA-02115, USA

[2]State Key Laboratory of Eco-hydraulics in Northwest Arid Region, Xi'an University of Technology, Xi'an, Shaanxi 710048, China

[3]Department of Civil and Environmental Engineering, University of Massachusetts-Amherst, Amherst MA-01002, USA

[4]Infrastructure and Environment Division, University of Glasgow, Glasgow G12 8LT, United Kingdom

[5]Civil and Environmental Engineering, Cornell University, Ithaca NY – 14853, USA

[*]**Corresponding Authors**

April Gu, Civil and Environmental Engineering, Cornell University (aprilgu@cornell.edu)

Abstract

Candidatus Accumulibacter phosphatis (CAP) and its sub-clades-level diversity has been associated and implicated in successful phosphorus removal performance in enhanced biological phosphorus removal (EBPR). Development of high-throughput untargeted methods to characterize clades of CAP in EBPR communities can enable a better understanding of Accumulibacter ecology at a higher-resolution beyond OTU-level in wastewater resource recovery facilities (WRRFs). In this study, for the first time, using integrated 16S rRNA gene sequencing, oligotyping and genome-resolved metagenomics, we were able to reveal clade-level differences in Accumulibacter communities and associate the differences with two different full-scale EBPR configurations. The results led to the identification and characterization of a distinct and dominant Accumulibacter oligotype - Oligotype 2 (belonging to Clade IIC) and its matching MAG (RC14) associated with side-stream EBPR configuration. We are also able to extract MAGs belonging to CAP clades IIB (RCAB4-2) and II (RC18) which did not have representative genomes before. This study demonstrates and validates the use of a high-throughput approach of oligotyping analysis of 16S rRNA gene sequences to elucidate CAP clade-level diversity. We also show the existence of a previously uncharacterized diversity of CAP clades in full-scale EBPR communities through extraction of MAGs, for the first time from full-scale facilities.

Introduction

Enhanced biological phosphorus removal (EBPR) has been a promising technology for phosphorus removal from municipal wastewater, due to its sustainable nature and P recovery potential in comparison to chemical precipitation and adsorption-based approaches [1]. However, conventional EBPR processes face challenges related to system stability and susceptibility to

variations and fluctuations in influent loading conditions such as unfavorable carbon to P (C/P) ratios [2]. A new emerging process, namely, side-stream EBPR (S2EBPR) features an anaerobic side-stream reactor that allows a portion of the return activated sludge (RAS) to undergo hydrolysis and fermentation thus enabling influent carbon-independent enrichment and selection of polyphosphate accumulation organisms (PAO). Facilities that have operated or piloted S2EBPR showed improved and more stable performance [3–6]. However, several key knowledge gaps still exist for this process including lack of understanding of the fundamental mechanisms governing the process and differences in microbial ecology, particularly functionally relevant key populations such as PAOs between the conventional and the S2EBPR processes. Several studies that have characterized the microbial ecology of different process configurations using 16S rRNA gene amplicon sequencing, fluorescence in-situ hybridization (FISH) and quantitative polymerase chain reaction (qPCR) have failed to associate differences in PAO microbial ecology with process configurations [7–10]. This is, at least partially due to the challenges in identification and association of specific PAO populations with various full-scale EBPR configurations. The complex and overwhelming “masking” effect of facility-specific selection forces exerted on the microbial community structure makes it difficult to isolate the effect of process configuration alone.

Candidatus (*Ca.*) Accumulibacter phosphatis (hereafter referred to as Accumulibacter or CAP) is considered to be a key PAO in both lab-scale and full-scale EBPR systems [11–16]. Our current understanding of the physiology, metabolic potential, transcriptional, and proteomic dynamics are based on lab-scale Accumulibacter-enriched reactors from which 19 metagenome-assembled genomes (MAGs) of Accumulibacter have been obtained [12, 16–20] and amongst them, only one complete draft genome sequence for Clade IIA, namely Accumulibacter UW1 has been

reported. These MAGs have highlighted the enormous genomic diversity in Accumulibacter clades (>700 unique genes in each clade) especially in terms of the capacity to perform the different steps of the denitrification pathway and ability to metabolize complex carbon sources [16]. However, besides the MAGs from lab-scale reactors, Accumulibacter genome assemblies from full-scale systems have not been reported, possibly due to their low relative abundance (< 5 % based on 16S rRNA gene sequencing) [10, 14] and insufficient depth of sequencing, which makes MAG extraction from metagenome assemblies difficult. Metagenomic studies have indicated high-level of diversity within Accumulibacter populations in full-scale EBPR communities [10, 14], however this diversity was not fully characterized due to the inability to extract high-quality MAGs. This phylogenetic diversity within Accumulibacter populations along with the genomic functional diversity across clades points towards ecological niche-partitioning due to determinants such as type of carbon source, phosphorus levels, length of anaerobic period, and presence of alternate electron acceptors such as nitrate and nitrite etc. Characterization of the microdiversity along with generation of corresponding MAGs could lead to a better understanding of the niche determinants of Accumulibacter ecology which would help better inform treatment process optimization and operation.

Current methods to characterize clade-level differences in Accumulibacter populations include qPCR, FISH, *ppk1* gene sequencing and metagenomic sequencing. qPCR and FISH have been extensively used to characterize the clade-level differences in lab-scale and full-scale systems [21–24]. However, they target only those currently known clades for which primers or probes are available. Metagenomic and *ppk1* gene sequencing are untargeted analyses and are capable of providing phylogenetic information, however they are cost-prohibitive and/or time-consuming for routine analysis at full-scale practice. Although, 16S rRNA gene amplicon sequencing has

emerged to be a high-throughput and widely-used method to characterize and capture broad shifts in microbial communities, it is recognized that it fails to capture the phylogenetic diversity within OTUs (also called microdiversity) [25, 26]. Recent studies have highlighted the importance of capturing this diversity and that genetic variation in 16S rRNA gene amplicon sequences can capture meaningful ecologically distinct units [27, 28]. Recent work has argued for the use of a higher similarity threshold [25, 26] or for the use of exact sequence variants (ESVs) or amplicon sequence variants (ASVs) [29, 30] to more accurately characterize the microdiversity in a community. Oligotyping has been proposed as a method that can distinguish meaningful sequence variation from sequencing errors and can partition sequence types that differ in as little as one nucleotide with the assumption that the variation in small regions of the 16S rRNA gene translate to phylogenetic differences [27, 28, 30].

In this study, we employed 16S rRNA gene sequencing, oligotyping and metagenomic analysis to elucidate and compare the microbial ecology and potential functional traits of Accumulibacter between conventional and S2EBPR process configurations in full-scale systems. The unique opportunity to operate two different EBPR configurations, in parallel and separate treatment trains with the same influent feed, made it possible to eliminate other influent characteristics-related selection factors and, therefore enabled association of specific CAP clades with S2EBPR versus conventional A2O configuration. To overcome the limitation of 16S rRNA gene sequencing and OTU-based approaches in revealing microdiversity, we demonstrated and validated the use of oligotyping in revealing the microdiversity within Accumulibacter populations. The results of the oligotyping analysis were further compared and confirmed with phylogenetic analysis of both full-length 16S rRNA and *ppk1* gene sequences retrieved from metagenomic sequencing. In addition, using differential coverage binning, we successfully

assembled and binned 2 high-quality and 1 medium-quality [31] Accumulibacter MAGs from full-scale EBPR sludge for the first time, including a distinct *Ca.* Accumulibacter clade that is dominant and associated with the S2EBPR configuration. Lastly, comparative genomic analysis was performed with the extracted MAGs and with previously published MAGs, to determine differences in key metabolic pathways and functions including unique functions that could contribute to niche-partitioning in the dynamic and complex environments in full-scale EBPR facilities.

Materials and Methods

Rock Creek Pilot

Full-scale testing was conducted from June 22nd to August 30th 2016 at the Rock Creek Facility (Hillsboro, Oregon). Two parallel trains with separated secondary clarifiers were operated with the same influent wastewater side-by-side, with one operated as conventional EBPR and another one as S2EBPR configuration for comparison. The S2EBPR configuration implemented was side-stream RAS fermentation with supplemental carbon addition (SSRC). In this configuration, 100% of the RAS was diverted to the side-stream reactor (Figure S1) for a total anaerobic HRT of 1.5 hours with primary sludge fermentate addition. The side-stream reactor was mixed intermittently once every week for 10 minutes during the sampling period for this study. The conventional EBPR configuration was an A2O process with an anaerobic HRT of 0.7 hours. Average influent flow to each treatment trains during the testing period was 5.35 MGD. Throughout the testing period, process performance parameters were routinely monitored. Detailed information on operation and performance is available in supplementary methods and published literature [4, 6, 32].

Sampling, DNA Extraction, Amplicon Sequencing and Analysis

Sampling was performed before pilot testing was started as a baseline (April 7th and April 26th, 2016) and during pilot testing (June 22nd, July 20th, August 2nd, August 17th, and August 30th, 2016). MLSS samples were collected at the end of the aerobic zone, shipped to Northeastern University, Boston MA overnight on dry ice. DNA was extracted according to the MiDAS protocol [33]. The extracted DNA was sent to University of Connecticut-MARS facility for PCR amplification and sequencing targeting the V4 region using the primers 515F (5'-GTGCCAGCMGCCGCGGTAA-3') and 806R (5'-GGACTACHVGGGTWTCTAAT-3') [34] and the amplicons were sequenced on the Illumina MiSeq using V2 chemistry using paired-end (2 X 250) sequencing [35]. Raw reads have been submitted to NCBI under the BioProject accession number PRJNA530271.

The sequences were trimmed to remove primers and barcodes, quality filtered using sickle v1.33 [36] with a minimum quality score of 20 and analyzed as described in Kozich et al., [35]. Consensus taxonomy of OTUs was determined using the 80% cugtoff using the MiDAS (v123) database [33] (details of the analysis are provided in the supplementary methods). Amplicon data was rarefied to the minimum total sequence count (12090 sequences) across all samples. All data and statistical analysis were performed in R (for more details see supplementary methods) using the following packages: vegan (Oksanen et al. 2007), ggplot2 [37], dplyr [38] and ampvis [39].

Oligotyping Analysis

To generate the input sequences required for oligotyping analysis, the Kozich et al., [35] pipeline, described above, was executed without the preclustering step as recommended by Eren et al. [30]. After chimera removal and denoising sequences, the 16S rRNA gene amplicon (V4 region) sequences classified as *Ca.* Accumulibacter were extracted and formatted as required by

the oligotyping pipeline using the mothur2oligo.sh script (https://github.com/michberr/MicrobeMiseq/tree/master/mothur2oligo). A total of 38855 sequences that were classified as *Ca.* Accumulibacter were extracted and used as input for oligotyping analysis. The oligotyping pipeline (v2.1) was used according to Eren et al. [30] with recommended best practices. Quality filtering in the oligotyping pipeline resulted in 37934 reads (97.6 %). The Shannon entropy at each nucleotide position was calculated using the entropy-analysis command. Starting with the highest entropy positions, 9 nucleotide positions (56, 57, 63, 75, 112, 113, 114, 115, 123) were selected for entropy decomposition (Figure S2). Noise filtering was performed by limiting our analysis to oligotypes that occurred in at least 3 samples (-s) and those that had a minimum count (-M) of 30 (~0.1 %). A total of 195 raw oligotypes were initially identified based on the 9 nucleotide positions. Denoising and elimination based on the -s and -M parameters resulted in 9 oligotypes.

Metagenomic Sequencing, Assembly and Genome Binning

Samples from June 26th, August 2nd and August 30th, 2016 from both treatment trains were sent to the TUCF Genomics center for 2 x 250 paired end sequencing on the Illumina HiSeq 2500. Library preparation for metagenomic sequencing was performed using the TruSeq PCR-free DNA kit. A total of 83.2 million paired-end reads were obtained. Sequences were quality filtered using sickle v1.33 [36] with a quality threshold of 20 and a length threshold of 50. In order to remove contamination sequences, the quality filtered sequences were then mapped to the UniVec database [40] and mapped reads were removed. Paired-end reads for all 6 samples were then co-assembled together using MEGAHIT [41] using a minimum contig length of 1000 to enable recovery of MAGs and eliminate erroneous contigs. Samples (n=3) from each treatment train were also co-assembled separately. Quality for the assemblies (total 3 assemblies) was assessed

using QUAST [42]. The paired-end reads obtained after Univec-filtering were mapped to the assemblies using Bowtie 2.0 [43]. The resulting sam files were converted to bam, sorted and indexed using samtools [44]. Duplicate reads were removed using Picard [45]. Assembled contigs were then classified using Kaiju [46] with the default database. Genome binning was performed using the CONCOCT [47] implementation in Anvi'o [48] with a cluster size of 350. Resulting bins with >70 % completion were then manually refined in Anvi'o based on coverage patterns, GC content and taxonomic affiliation. The quality of all refined bins was then assessed with CheckM v1.0.11 and taxonomic classification was also obtained. Genome bins from the different assemblies were dereplicated using dRep [49] and the dereplicated bins were then used for downstream analysis. Bins, classified as *Rhodocyclaceae*, were extracted and paired-end reads from each sample were mapped against the MAGs using bbmap (v37.78) with 90% minimum identity while choosing only the best hit and matching paired-end reads. Contig-wise coverage was calculated using the pileup.sh script (https://github.com/BioInfoTools/BBMap/blob/master/sh/pileup.sh). Relative abundance of genome bins was calculated using the following equation (assuming an average genome length of 6 Mbp):

$$Relative\ abundance = \frac{\frac{No.of\ Reads\ Mapped_{Bin}}{Length\ Mapped_{Bin}}}{\frac{No.of\ Reads\ Mapped_{Assembly}}{Average\ Genome\ Length}}$$

Raw reads and identified Accumulibacter MAG assemblies have been submitted to NCBI and are accessible under the BioProject accession number PRJNA530189.

Reconstruction of full-length 16S rRNA Gene Sequences

EMIRGE [50] was used to reconstruct 16S rRNA gene sequences from the paired-end metagenomic data. Exact sequence matches to oligotypes were extracted, aligned with the reference sequences from He et al., [21] and a phylogenetic analysis was performed using MrBayes 3.2 [51] (see supplementary methods for details).

ppk1 Annotation and Phylogenetic Analysiss

ppk1 genes were annotated in the assemblies using a HMM model [52] using HMMER 3.1b2 (http://hmmer.org/). The annotated genes were then aligned with the reference sequences (n=1012) using MUSCLE v3.8.31 [53] and placed on a reference backbone tree using pplacer [54]. Read counts for each of the identified ppk1 sequences were obtained using the multicov tool in BEDtools [55] and the reads per kilobase million (RPKM) value was calculated. Sequences with length less than 600 bp were filtered out and relative abundance of the *ppk1* gene sequences was calculated using the following equation:

$$relative\ abundance = \frac{RPKM_{ppk1\ sequence}}{sum(RPKM)_{sample}}$$

Pangenomic and Phylogenetic Analysis

All publicly available genomes for *Ca.* Accumulibacter (n=19) were downloaded and combined with the CAP MAGs obtained in this study to perform a pangenomic analysis using the Anvi'o 5.1 [48] pangenomic workflow. Functional annotation of the MAGs was performed using GhostKOALA [56]. A set of 37 marker genes were identified using Phylosift and a concatenated alignment of these were used to construct a maximum-likelihood (ML) tree in RaxML version 8.2.11 [57] with a 100 bootstraps and with GTRGAMMA settings. For the phylogenetic analysis, published *Propionivibrioeu* (*Propionivibrio dixarboxylicus*, *Propionivibrio militaris*, *Ca.*

Propionivibrio aalborgensis) and *Dechloromonas aromatica* RCB genomes were used as outgroups. The best-scoring ML tree was used. The *ppk1* gene was also annotated in all the genomes and used for a phylogenetic analysis using pplacer as outlined previously.

Results and Discussion

No observed differences in Accumulibacter diversity and relative abundance were observed at genus or OTU-level between conventional A2O and S2EBPR SSRC configurations

In this study, Accumulibacter was found to be the most abundant PAO in both EBPR configurations (Figure S2) [4, 6]. The estimated relative abundance of Accumulibacter, based on 16S rRNA gene sequencing, increased from the start of the pilot (June 21st, 2016) until the end (August 30th, 2016) in both treatment trains from an average abundance of 0.35 ± 0.05 % (both conventional and S2EBPR) to 1.98 ± 0.12 % (both conventional and S2EBPR) [4, 6]. A genus-level analysis did not reveal significant differences between the two EBPR configurations in the diversity and relative abundance of putative PAOs such as Accumulibacter. At the OTU-level, both treatment trains showed a predominance of OTU 00015 with most of the total Accumulibacter relative abundance accounted for by OTU 00015 (Figure 1). The rest of the OTUs were present at very low relative abundances. The results suggested that the diversity in Accumulibacter populations, if any, could not be resolved using OTU-based methods. However, there is still potential for finer-resolution diversity which could be masked within the OTUs.

Oligotyping reveals differences in Accumulibacter clades between S2EBPR SSRC and conventional A2O configurations

In order to further resolve the microdiversity within Accumulibacter OTUs, oligotyping analysis was performed using the individual 16S rRNA gene sequences targeting the V4 region. The oligotyping analysis enabled the identification of 9 oligotypes of Accumulibacter and therefore

243 distinct Accumulibacter community structure between the two EBPR configurations. The
244 S2EBPR Accumulibacter community became increasingly dominated by Oligotype 2, during the
245 testing period, while it remained at a very low relative abundance in the conventional A2O
246 configuration (Figure 2A, Table S1). The relative abundance of Oligotype 2 increased from 31.8
247 ± 8.1 % at the start of testing (Jun 22) to 68.0 ± 0.2 % on Aug 17th and 62.4 ± 1.3 % on Aug
248 30th in S2EBPR while it remained below 20 % of the Accumulibacter sequences in the parallel
249 conventional A2O treatment trains. The continuously increasing abundance of the Oligotype 2 in
250 S2EBPR over a time-series and its consistently low abundance in A2O suggests that this
251 oligotype was most likely favored and enriched by conditions in the S2EBPR configuration. In
252 comparison, predominant oligotypes in A2O were Oligotypes 5 and 6 (Figure 2A). A
253 hierarchical clustering analysis of the samples based on the oligotyping data showed distinct
254 clusters based on operating regime (Figure S4). All samples from the S2EBPR train clustered
255 together except for the sample from June 22nd which was the date when the piloting was started.
256 Samples from A2O taken during the later stages of piloting (Aug 17th, Aug 30th) clustered
257 together while the ones during the earlier stages (Jun 22nd, Jul 20th, and Aug 2nd) clustered
258 separately.

259 ***Phylogenetic analysis of oligotype sequences shows congruency with ppk1-phylogeny of***
260 ***Accumulibacter***

261 In order to further correlate the oligotypes to clade/species level differences in CAP and examine
262 the congruency of the oligotype phylogeny with *ppk1* phylogeny, we performed phylogenetic
263 analysis using near full-length 16S rRNA gene and *ppk1* sequences through metagenomic
264 sequencing on the samples taken on June 22nd, August 2nd, and August 30th from both
265 treatment trains. A phylogenetic analysis of near full-length 16S rRNA gene sequences

(extracted from metagenomic sequencing), classified as Accumulibacter and matching 5 of 9 oligotypes, along with reference sequences from He et al., [21], which were previously assigned to clades based on congruency with *ppk1* phylogeny, revealed that the 16S rRNA gene sequences matching the oligotypes were monophyletic (Figure 2B). It is important to note that multiple full-length 16S rRNA gene sequences with identical V4 regions matching each oligotype were obtained and they all clustered within the same clade. The sequences matching Oligotype 2, which is the dominant oligotype in S2EBPR, clustered with Clade IIC/D 16S rRNA gene sequences (He et al., 2007). Oligotype 6 clustered with Clade Clade IIA 16S rRNA gene sequences. Oligotype 5 did not cluster with any representative 16S rRNA reference sequence at a sub-clade level, but clustered with Clade II sequences. This could be due to the lack of a representative reference sequences for that particular sub-clade.

Sub-clades within Accumulibacter has been previously resolved using the *ppk1* gene [17, 58–61]. A phylogenetic analysis of *ppk1* gene sequences, extracted from metagenomic sequencing and assigned clades using pplacer (Figure S5), was performed and the cumulative relative abundance of sequences belonging to each clade was calculated (Figure 2C). This further confirmed that Clade IIC was predominant in S2EBPR which is congruent with oligotyping results. However, according to *ppk1* phylogeny, Clade IIG was the predominant clade in the conventional A2O configuration at the end of testing which was not directly congruent with the results using 16S rRNA oligotyping phylogeny. This could be due to the lack of representative 16S rRNA gene reference sequences for Clade IIG.

Previous research has cautioned that exact sequence variants (ESVs) or oligotypes may not represent phylogenetically or ecologically significant units [62]. However, this was based on a study of *Microcystis* in freshwater systems where they observed that the oligotypes observed in

the study were not monophyletic and did not correlate with toxin producing capability. In this study, we show that the dominant oligotypes observed are distinct between EBPR configurations fed with the same influent wastewater and their full-length 16S rRNA gene sequence matches from metagenomic reconstruction are monophyletic. Furthermore, we show that the oligotyping results agree with the phylogenetic analysis with a more robust marker gene (*ppk1*) for Accumulibacter. It should be noted that, until now, the only way to resolve clade-level differences in Accumulibacter has been using the *ppk1* gene or using metagenomics. Even though qPCR primers for the *ppk1* gene exist for many clades, it is unclear whether these capture the diversity of Accumulibacter sufficiently. The potential advantages of resolving clade-level differences using a high-throughput method such as 16S rRNA gene amplicon sequencing combined with oligotyping is significant since it will enable more cost-effective and improved characterization of EBPR communities. However, the use of this method needs to be further validated by comparing with other tools that can differentiate closely-related taxa in order to characterize the microdiversity in a particular taxon.

Accumulibacter MAGs binned from the metagenomic sequences reveal previously uncharacterized diversity in full-scale EBPR systems

To further characterize the identity and metabolic capabilities of Accumulibacter present in the two full-scale EBPR systems with different configurations, we used genome-resolved metagenomics to recover 3 MAGs (RC14, RC18, and RCAB4-2) classified putatively as Accumulibacter. The taxonomic affiliation of these MAGs was further delineated by performing a phylogenomic analysis along with 19 published Accumulibacter MAGs [13, 17, 18, 20, 63] using a concatenated alignment of 37 single-copy genes (SCG). Based on the SCG phylogeny (Figure s3A), the three MAGs were confirmed to be affiliated with Accumulibacter. RC14 and

RC18 were high-quality MAGs with a completion of 99 % and 98.2 % respectively with low redundancy values of 0.2 % and 0.0 % respectively. The other MAG (RCAB4-2) had a completion of 77.2% and 3.1% redundancy.

To further delineate the clade-level taxonomy of the MAGs, the *ppk1* gene sequence from each MAG was extracted and placed on the reference tree as described previously. Based on their placement (Figure s3B), MAG RC14 can be classified as Clade IIC and RCAB4-2 as Clade IIB. Based on both SCG and *ppk1* phylogeny, MAG RC18 does not cluster under any of the canonical groupings at the sub-clade level, which suggests that it is a previously uncharacterized sub-clade of Accumulibacter since MAGs from full-scale facilities have not been published before. Both the SCG and *ppk1* phylogeny, suggest that RC18 would belong to Clade II. Average nucleotide identity (ANI) was used to confirm the results of the phylogenetic analysis (Figure S7). MAG RC14 had a > 90% ANI with Clade IIC MAGs over an alignment fraction of 57.0 % (BA91), 75.3 % (HKU2), 62 % (SK01), 70.8 % (SK02) and 72 % (UBA5574). This would confirm the classification of RC14 as a Clade IIC genome [64]. MAG RC18 and RCAB4-2 had an alignment fraction of < 10 % and < 20 % respectively with any of the other MAGs with ANIs of < 85 % again reinforcing the results of the phylogenetic analysis that these are previously uncharacterized clades [64]. We also calculated the relative abundance of these MAGs in the metagenome and observed that RC14 (Clade IIC) was the predominant Accumulibacter MAG in the S2EBPR metagenome (Figure 3C). Note that the clade affiliation of these genome bins corresponds to the predominant clades observed using both oligotyping and *ppk1* annotation (Figure 2). Clade IIC MAG (RC14) was the most abundant Accumulibacter MAG in S2EBPR, thus, again, confirming the oligotyping approach for resolving the microdiversity within CAP phylogeny.

The newly identified RC18 genome seems to belong to a previously uncharacterized clade while RCAB4-2 is classified as Clade IIB for which there have not been any representative MAGs published. Our results revealed and highlighted the as-yet uncharacterized diversity of Accumulibacter. Particularly, draft genomes from full-scale systems have previously not been published, therefore the MAGs obtained in this study could expand the current knowledge on the genomic diversity in Accumulibacter in full-scale EBPR systems.

Comparative Genomics of Ca. Accumulibacter

A comparative genomic analysis of 3 CAP MAGs obtained in this study along with 19 published CAP MAGs was performed with a focus on pathways relevant to EBPR metabolism such as polyP metabolism, phosphate transporters, carbon cycling, and denitrification (Figure 4).

Core EBPR Metabolism

The characteristic metabolism of PAOs in EBPR is the concurrent cycling of carbon and phosphorus through storage and use of intracellular polymers such as glycogen, polyhydroxyalkanoates (PHA) and polyphosphate (polyP). The MAGs extracted in this study (RC14, RC18 and RCAB4-2) were annotated with all genes (Figure 4 & Table S3) considered essential for phosphate transport and polyP metabolism, including *pstSCAB, pitA, ppk1*, *ppk2* and *ppx*. It has been postulated that the presence of the low-affinity Pit transporter is vital to the PAO-phenotype [65]. The concerted action of these enzymes has been shown to be essential for the PAO phenotype and are present in all Accumulibacter MAGs including the three identified in this study [66, 67]. Genes for PHA synthesis, glycolysis and TCA cycle from both acetyl-CoA and propionyl-CoA were shared among all the MAGs. One of the debated features of the carbon metabolism in Accumulibacter is whether anaerobic glycolysis proceeds via the ED or the EMP pathway [68]. The consistent presence of the EMP pathway and the absence of genes for the ED

pathway in the currently available 22 MAGs of Accumulibacter, including 3 MAGs from full-scale facilities in this study, suggests that the EMP pathway is likely the predominant metabolism for anaerobic glycolysis (Figure 4 & Table S3). Another uncertainity in the anaerobic metabolism of EBPR is the source of the reducing equivalents for PHA formation under anaerobic conditions. Current hypothesized pathways include glycolysis, anaerobic operation of the TCA cycle, glyoxylate shunt and split TCA cycle [69–71]. Key enzymes for all these proposed pathways are present in the 3 MAGs from this study (Figure 4). This along with trancriptomic evidence from literature [11, 15, 18, 72, 73] suggests that Accumulibacter likely possess phenotypic versatility and can utilize various pathways in various combinations, depending on the availability of external substrate and intracellular polymers, for their anaerobic metabolism [71, 74, 75].

Carbon Metabolism

One of the critical aspects of PAO-type metabolism is the uptake of low molecular weight compounds such as VFAs (primarily acetate and propionate) under anaerobic conditions to form PHA. The 3 Accumulibacter MAGs, obtained in this study, contain the genes necessary for passive transport of acetate and propionate (*actP*) and conversion of acetate and propionate into acetyl-CoA and propionyl-CoA through acetate-coA synthetase (*acsA*) and propionate-coA ligase (*prpE*) respectively (Figure 4 & Table S3).

Full-scale facilities contain a variety of substrates in the wastewater including complex substrates, therefore the ability to use complex substrates can provide a niche for a PAO in full-scale facilities. Most of the MAGs of Accumulibacter, including the 3 MAGs from this study, encode a lactate dehydrogenase gene (*dld*) (except for BA94 and SK01) which catalyzes the conversion of lactate to pyruvate and the reverse reaction. The lactate permease gene (*lctP*/lldP)

was identified in aalborgensis, BA91, HKU2, UW1, RC18 and RCAB4-2. The presence of the lactate permease gene, in combination with lactate dehydrogenase, could confer the ability to uptake lactate and convert into pyruvate, acetyl-CoA or propionyl-CoA which can then be used to form PHB/PHV or feed the TCA cycle. Conversion of lactate to pyruvate is able to generate electron equivalents which can also be used for other active transport processes. A recent study [76] showed that Accumulibacter is capable of using lactate to store PHA, however, the authors noticed a deterioration in EBPR performance when feeding lactate presumably associated with a metabolic shift in Accumulibacter from utilizing both polyP and glycogen to utilizing just glycogen (similar to GAOs) since the use of lactate doesn't require the hydrolysis of polyP to generate ATP.

Nitrogen Metabolism

Another trait of interest in Accumulibacter metabolism is the ability to use various oxidized nitrogen species as electron acceptors. Among the available MAGs, only those in Clade IIC MAGs, including MAG RC14 that was dominant in the S2EBPR configuration in this study and one exception from IIA (aalborgensis), contain gene sets for respiratory nitrate reduction (*narGHI*) and nitrite reduction (*nirS*), but did not possess genes for subsequent steps of denitrification. The only MAG that contains genes for a complete denitrification pathway is UW-LDO-IC (Clade IC). Recent work with metatranscriptomics [20] showed that under micro-aerobic conditions and in the presence of nitrate, UW-LDO-IC is able to use both nitrate and oxygen simultaneously as electron acceptors even though the ability to use nitrate as an electron acceptor with exclusive and concurrent uptake of phosphate was not shown.

Most other clades (Clade IIA, IIB, IIF, IA, and IB) contain genes for periplasmic dissimilatory nitrate reduction (*napAB*) system. The Nap system is generally considered to not be coupled with

PMF generation and anaerobic respiration. It has been suggested that this system might be involved in aerobic denitrification for roles in adaptation to anaerobic metabolism after transition from aerobic conditions such as in EBPR [78]. There is also evidence that Nap is a dissimilatory enzyme used for optimizing redox balancing [79, 80]. The possession of periplasmic Nap system enzymes in majority of the Accumulibacter clades seem to suggest that these Accumulibacter likely do not use nitrate as an electron acceptor for respiration and denitrification. Rather, the Nap system likely allows CAPs to aerobically reduce nitrate to nitrite in the periplasm, which can be utilized for downstream nitrite reduction or excreted outside the cell.

It is possible that Accumulibacter species with truncated denitrification pathways could use complementary pathways in flanking populations to perform complete denitrification on a community level [77]. Presence of genes for nitric oxide reduction are restricted to a few MAGs in Clade II (UW1, RCAB4-2, BA91) and most Clade I MAGs. In contrast, genes for nitrous oxide reduction are present in almost all Clade IIF, Clade I MAGs and UW1 (Clade IIA). Noticeably, RC18 (present in both the conventional and S2EBPR full-scale systems) did not possess any of the reductases in the denitrification pathway, despite having a completion of 98.2 %.

Unique Functions in MAGs from Full-Scale Systems

In this study, we were able to obtain 3 Accumulibacter MAGs from full-scale EBPR communities. It is likely that MAGs from full-scale facilities have some unique functional abilities compared to MAGs from enriched lab-scale bioreactors to enable the organism to survive in the highly dynamic and complex environmental conditions in wastewater treatment systems. We identified genes for dimethyl sulfoxide (DMSO) reduction exclusively in RC18. The pathway included the *dmsA* and *dmsB* subunits of the *dmsABC* gene cluster. The DMSO

427 respiratory pathway has been extensively studied in photo-heterotrophic organisms such as
428 *Rhodobacter* spp. and plays a role in the organism's redox homeostasis and enables the
429 organisms to utilize a diversity of carbon sources during dark anaerobic growth [80]. Its potential
430 role in Accumulibacter metabolism is unknown and warrants further investigation. We also
431 identified the gene for alkane oxidation, alkane 1-monooxygenase (*alkB*) in RCAB4-2. The
432 production of this enzyme enables the oxidation of alkanes to alcohols making it an important
433 enzyme for bioremediation of petroleum hydrocarbon contaminated environments [81, 82].
434 Whether this enzyme has a direct impact on EBPR metabolism is unknown.

435 In this study, for the first time, using integrated amplicon sequencing, oligotyping and genome-
436 resolved metagenomics, we were able to reveal clade-level differences in Accumulibacter
437 communities and associate the differences with two different full-scale EBPR configurations.
438 The results led to the identification and characterization of a distinct and dominant
439 Accumulibacter oligotype - Oligotype 2 (belonging to Clade IIC) and its matching MAG (RC14)
440 associated with S2EBPR configuration. This study demonstrates that oligotyping of the V4
441 region of the 16S rRNA gene could resolves clade-level differences, congruent with *ppk1*-
442 phylogeny, in Accumulibacter communities in full-scale EBPR systems. The potential
443 advantages of resolving clade-level differences using a high-throughput method such as 16S
444 rRNA gene amplicon sequencing combined with oligotyping is significant since it will enable
445 wider capture, higher-resolution and more cost-effective genotyping of Accumulibacter
446 communities and thus improve our ability to characterize and monitor EBPR processes.
447 Genome-resolved metagenomics also enabled us to retrieve 3 new CAP MAGs from full-scale
448 facilities including two MAGs, RCAB4-2 and RC18, belonging to Clade IIB and to a previously
449 uncharacterized sub-clade of Clade II respectively, that did not have any previous representative

450 genomes. Comparative genomics of the obtained MAGs showed unique functions that could
451 enable niche-partitioning of particular clades under different conditions.

452 ## Acknowledgements

453 Funding for this research was provided by the Water Environment & Reuse Foundation (Project
454 No: U1R13), Hampton Roads Sanitation District, and Woodard & Curran, Inc. The authors thank
455 Peter Schauer, Adrienne Menniti and Chris Maher (Clean Water Services) for their assistance in
456 this study.

457 ## Conflict of Interest

458 The authors declare no conflict of interest.
459

460 ## References
461

462 1. Morse GK, Brett SW, Guy JA, Lester JN. Review: Phosphorus removal and recovery
463 technologies. *Sci Total Environ* 1998; **212**: 69–81.

464 2. Gu AZ, Saunders A, Neethling JB, Stensel HD, Blackall LL. Functionally Relevant
465 Microorganisms to Enhanced Biological Phosphorus Removal Performance at Full-Scale
466 Wastewater Treatment Plants in the United States. *Water Environ Res* 2008; **80**: 688–698.

467 3. Onnis-Hayden A, Srinivasan V, Tooker NB, Li G, Wang D, Gu AZ. Survey of Full Scale
468 Side-Stream EBPR Facilities and Comparison with Conventional EBPR: Process Stability,
469 Kinetics and Microbial Ecology. *Preprints* 2018.

470 4. Gu AZ, Tooker NB, Onnis-Hayden A, Wang D, Srinivasan V, Li G, et al. Optimization
471 and Design of a Side-Stream EBPR Process as a Sustainable Approach for Achieving
472 Stable and Efficient Phosphorus Removal. 2019.

5. Barnard JL, Kobylinski E. The Case for Side-Stream RAS or Mixed Liquor Fermentation To Enhance Biological Phosphorus Removal (EBPR). *Proc. Water Environ. Fed. Nutr.* 2018. Raleigh, NC.

6. Wang D, Tooker NB, Srinivasan V, Li G, Schauer P, Menniti A, et al. A Full-Scale Comparative Study of Conventional and Side-Stream Enhanced Biological Phosphorus Removal Processes. *Preprints* 2018.

7. Mielczarek AT, Nguyen HTT, Nielsen JL, Nielsen PH. Population dynamics of bacteria involved in enhanced biological phosphorus removal in Danish wastewater treatment plants. *Water Res* 2013; **47**: 1529–1544.

8. Stokholm-Bjerregaard M, McIlroy SJ, Nierychlo M, Karst SM, Albertsen M, Nielsen PH. A Critical Assessment of the Microorganisms Proposed to be Important to Enhanced Biological Phosphorus Removal in Full-Scale Wastewater Treatment Systems. *Front Microbiol* 2017; **8**: 718.

9. Flowers JJ, Cadkin TA, McMahon KD. Seasonal bacterial community dynamics in a full-scale enhanced biological phosphorus removal plant. *Water Res* 2013; **47**: 7019–7031.

10. Law Y, Kirkegaard RH, Cokro AA, Liu X, Arumugam K, Xie C, et al. Integrative microbial community analysis reveals full-scale enhanced biological phosphorus removal under tropical conditions. *Sci Rep* 2016; **6**: 25719.

11. Oyserman BO, Noguera DR, del Rio TG, Tringe SG, McMahon KD. Metatranscriptomic insights on gene expression and regulatory controls in Candidatus Accumulibacter phosphatis. *ISME J* 2016; **10**: 810–822.

494 12. Martín HG, Ivanova N, Kunin V, Warnecke F, Barry KW, McHardy AC, et al.
495 Metagenomic analysis of two enhanced biological phosphorus removal (EBPR) sludge
496 communities. *Nat Biotechnol* 2006; **24**: 1263–1269.

497 13. Flowers JJ, He S, Malfatti S, del Rio TG, Tringe SG, Hugenholtz P, et al. Comparative
498 genomics of two 'Candidatus Accumulibacter' clades performing biological phosphorus
499 removal. *ISME J* 2013; **7**: 2301–2314.

500 14. Albertsen M, Hansen LBS, Saunders AM, Nielsen PH, Nielsen KL. A metagenome of a
501 full-scale microbial community carrying out enhanced biological phosphorus removal.
502 *ISME J* 2012; **6**: 1094–1106.

503 15. Barr JJ, Dutilh BE, Skennerton CT, Fukushima T, Hastie ML, Gorman JJ, et al.
504 Metagenomic and metaproteomic analyses of Accumulibacter phosphatis-enriched
505 floccular and granular biofilm. *Environ Microbiol* 2016; **18**: 273–287.

506 16. Skennerton CT, Barr JJ, Slater FR, Bond PL, Tyson GW. Expanding our view of genomic
507 diversity in *Candidatus* Accumulibacter clades. *Environ Microbiol* 2015; **17**: 1574–1585.

508 17. Albertsen M, McIlroy SJ, Stokholm-Bjerregaard M, Karst SM, Nielsen PH. '*Candidatus*
509 Propionivibrio aalborgensis': A novel glycogen accumulating organism abundant in full-
510 scale enhanced biological phosphorus removal plants. *Front Microbiol* 2016; **7**.

511 18. Mao Y, Yu K, Xia Y, Chao Y, Zhang T. Genome reconstruction and gene expression of '
512 candidatus accumulibacter phosphatis' Clade IB performing biological phosphorus
513 removal. *Environ Sci Technol* 2014; **48**: 10363–10371.

514 19. Camejo PY, Oyserman BO, McMahon KD, Noguera DR. Integrated Omic Analyses

Provide Evidence that a " *Candidatus* Accumulibacter phosphatis" Strain Performs Denitrification under Microaerobic Conditions. *mSystems* 2019; **4**: 1–23.

20. Parks DH, Rinke C, Chuvochina M, Chaumeil PA, Woodcroft BJ, Evans PN, et al. Recovery of nearly 8,000 metagenome-assembled genomes substantially expands the tree of life. *Nat Microbiol* 2017; **2**: 1533–1542.

21. He S, Gall DL, McMahon KD. 'Candidatus accumulibacter' population structure in enhanced biological phosphorus removal sludges as revealed by polyphosphate kinase genes. *Appl Environ Microbiol* 2007; **73**: 5865–5874.

22. Camejo PY, Owen BR, Martirano J, Ma J, Kapoor V, Santo Domingo J, et al. Candidatus Accumulibacter phosphatis clades enriched under cyclic anaerobic and microaerobic conditions simultaneously use different electron acceptors. *Water Res* 2016; **102**: 125–137.

23. Welles L, Abbas B, Sorokin DY, Lopez-Vazquez CM, Hooijmans CM, van Loosdrecht MCM, et al. Metabolic response of '*Candidatus* Accumulibacter phosphatis' clade IIC to changes in influent P/C ratio. *Front Microbiol* 2017; **7**.

24. Mao Y, Graham DW, Tamaki H, Zhang T. Dominant and novel clades of Candidatus Accumulibacter phosphatis in 18 globally distributed full-scale wastewater treatment plants. *Sci Rep* 2015; **5**: 11857.

25. Edgar RC. Updating the 97% identity threshold for 16S ribosomal RNA OTUs. *Bioinformatics* 2018; 1–5.

26. Chase AB. The importance of resolving biogeographic patterns of microbial

536 microdiversity. *Microbiol Aust* 2018; 18–21.

537 27. Fisher JC, Murat Eren A, Green HC, Shanks OC, Morrison HG, Vineis JH, et al.
538 Comparison of sewage and animal fecal microbiomes by using oligotyping reveals
539 potential human fecal indicators in multiple taxonomic groups. *Appl Environ Microbiol*
540 2015; **81**: 7023–7033.

541 28. Fisher JC, Levican A, Figueras MJ, McLellan SL. Population dynamics and ecology of
542 Arcobacter in sewage. *Front Microbiol* 2014; **5**: 1–9.

543 29. Callahan BJ, McMurdie PJ, Holmes SP. Exact sequence variants should replace
544 operational taxonomic units in marker gene data analysis. *bioRxiv* 2017; 113597.

545 30. Eren AM, Maignien L, Sul WJ, Murphy LG, Grim SL, Morrison HG, et al. Oligotyping:
546 Differentiating between closely related microbial taxa using 16S rRNA gene data.
547 *Methods Ecol Evol* 2013; **4**: 1111–1119.

548 31. Bowers RM, Kyrpides NC, Stepanauskas R, Harmon-Smith M, Doud D, Reddy TBK, et
549 al. Minimum information about a single amplified genome (MISAG) and a metagenome-
550 assembled genome (MIMAG) of bacteria and archaea. *Nat Biotechnol* 2017; **35**: 725–731.

551 32. Maher C, Schauer P, Menniti A. Testing the Limits of EBPR for Stable Operation. *Proc.*
552 *Water Environ. Fed. WEFTEC*. 2018. Chicago, IL, pp 1581–1594.

553 33. McIlroy SJ, Saunders AM, Albertsen M, Nierychlo M, McIlroy B, Hansen AA, et al.
554 MiDAS: The field guide to the microbes of activated sludge. *Database* 2015; **2015**: 1–8.

555 34. Caporaso JG, Lauber CL, Walters WA, Berg-Lyons D, Lozupone CA, Turnbaugh PJ, et
556 al. Global patterns of 16S rRNA diversity at a depth of millions of sequences per sample.

PNAS 2011; **108**: 4516–4522.

35. Kozich JJ, Westcott SL, Baxter NT, Highlander SK, Schloss PD. Development of a dual-index sequencing strategy and curation pipeline for analyzing amplicon sequence data on the miseq illumina sequencing platform. *Appl Environ Microbiol* 2013; **79**: 5112–5120.

36. Joshi N, Fass J. Sickle: A sliding-window, adaptive, quality-based trimming tool for FastQ files (Version 1.33) [Software]. *Available at https://github.com/najoshi/sickle* . 2011. , 2011

37. Wickham H. ggplot2: Elegant graphics for data analysis. 2009. Springer-Verlag, New York.

38. Wickman H, Francois R, Henry L, Müller K. A Grammar of Data Manipulation. R package version 0.7.5. 2018.

39. Albertsen M, Karst SM, Ziegler AS, Kirkegaard RH, Nielsen PH. Back to basics - The influence of DNA extraction and primer choice on phylogenetic analysis of activated sludge communities. *PLoS One* 2015; **10**: e0132783.

40. Univec database at National Center for Biotechnology Information [http://www.ncbi.nlm.nih.gov/VecScreen/UniVec.html].

41. Li D, Liu CM, Luo R, Sadakane K, Lam TW. MEGAHIT: An ultra-fast single-node solution for large and complex metagenomics assembly via succinct de Bruijn graph. *Bioinformatics* 2015; **31**: 1674–1676.

42. Mikheenko A, Saveliev V, Gurevich A. MetaQUAST: Evaluation of metagenome assemblies. *Bioinformatics* 2016; **32**: 1088–1090.

578 43. Langmead B, Salzberg SL. Fast gapped-read alignment with Bowtie 2. *Nat Methods* 2012;
579 **9**: 357–359.

580 44. Li H, Handsaker B, Wysoker A, Fennell T, Ruan J, Homer N, et al. The Sequence
581 Alignment/Map format and SAMtools. *Bioinformatics* 2009; **25**: 2078–2079.

582 45. Picard. http://broadinstitute.github.io/picard/.

583 46. Menzel P, Ng KL, Krogh A. Fast and sensitive taxonomic classification for metagenomics
584 with Kaiju. *Nat Commun* 2016; **7**: 11257.

585 47. Alneberg J, Bjarnason BS, de Bruijn I, Schirmer M, Quick J, Ijaz UZ, et al. Binning
586 metagenomic contigs by coverage and composition. *Nat Methods* 2014; **11**: 1144–1146.

587 48. Eren AM, Esen ÖC, Quince C, Vineis JH, Morrison HG, Sogin ML, et al. Anvi'o: an
588 advanced analysis and visualization platform for 'omics data. *PeerJ* 2015; **3**: e1319.

589 49. Olm MR, Brown CT, Brooks B, Banfield JF. DRep: A tool for fast and accurate genomic
590 comparisons that enables improved genome recovery from metagenomes through de-
591 replication. *ISME J* 2017; **11**: 2864–2868.

592 50. Miller CS, Baker BJ, Thomas BC, Singer SW, Banfield JF. EMIRGE: Reconstruction of
593 full-length ribosomal genes from microbial community short read sequencing data.
594 *Genome Biol* 2011; **12**.

595 51. Ronquist F, Huelsenbeck JP. MrBayes 3: Bayesian phylogenetic inference under mixed
596 models. *Bioinformatics* 2003; **19**: 1572–1574.

597 52. Leventhal GE, Boix C, Kuechler U, Enke TN, Sliwerska E, Holliger C, et al. Strain-level
598 diversity drives alternative community types in millimetre-scale granular biofilms. *Nat*

Microbiol 2018; **3**: 1295–1303.

53. Edgar RC. MUSCLE: multiple sequence alignment with high accuracy and high throughput. *Nucleic Acids Res* 2004; **32**: 1792–1797.

54. Matsen FA, Kodner RB, Armbrust EV. pplacer: linear time maximum-likelihood and Bayesian phylogenetic placement of sequences onto a fixed reference tree. *BMC Bioinformatics* 2010; **11**: 538.

55. Quinlan AR, Hall IM. BEDTools: a flexible suite of utilities for comparing genomic features. *Bioinformatics* 2010; **26**: 841–842.

56. Kanehisa M, Sato Y, Morishima K. BlastKOALA and GhostKOALA: KEGG Tools for Functional Characterization of Genome and Metagenome Sequences. *J Mol Biol* 2016; **428**: 726–731.

57. Stamatakis A. RAxML version 8: A tool for phylogenetic analysis and post-analysis of large phylogenies. *Bioinformatics* 2014; **30**: 1312–1313.

58. McMahon KD, Yilmaz S, He S, Gall DL, Jenkins D, Keasling JD. Polyphosphate kinase genes from full-scale activated sludge plants. *Appl Microbiol Biotechnol* 2007; **77**: 167–173.

59. Skennerton CT, Barr JJ, Slater FR, Bond PL, Tyson GW. Expanding our view of genomic diversity in *Candidatus* Accumulibacter clades. *Environ Microbiol* 2015; **17**: 1574–1585.

60. Camejo PY, Oyserman BO, McMahon KD, Noguera DR. Integrated Omic Analyses Provide Evidence that a " *Candidatus* Accumulibacter phosphatis" Strain Performs Denitrification under Microaerobic Conditions. *mSystems* 2019; **4**.

620 61. He S, Gu AZ, McMahon KD. Progress toward understanding the distribution of
621 Accumulibacter among full-scale enhanced biological phosphorus removal systems.
622 *Microb Ecol* 2008; **55**: 229–236.

623 62. Berry MA, White JD, Davis TW, Jain S, Johengen TH, Dick GJ, et al. Are oligotypes
624 meaningful ecological and phylogenetic units? A case study of Microcystis in Freshwater
625 lakes. *Front Microbiol* 2017; **8**: 1–7.

626 63. Skennerton CT, Barr JJ, Slater FR, Bond PL, Tyson GW. Expanding our view of genomic
627 diversity in CandidatusAccumulibacter clades. *Environ Microbiol* 2015; **17**: 1574–1585.

628 64. Varghese NJ, Mukherjee S, Ivanova N, Konstantinidis KT, Mavrommatis K, Kyrpides
629 NC, et al. Microbial species delineation using whole genome sequences. *Nucleic Acids*
630 *Res* 2015; **43**: 6761–6771.

631 65. McIlroy SJ, Albertsen M, Andresen EK, Saunders AM, Kristiansen R, Stokholm-
632 Bjerregaard M, et al. 'Candidatus Competibacter'-lineage genomes retrieved from
633 metagenomes reveal functional metabolic diversity. *ISME J* 2014; **8**: 613–624.

634 66. Kristiansen R, Nguyen HTT, Saunders AM, Nielsen JL, Wimmer R, Le VQ, et al. A
635 metabolic model for members of the genus *Tetrasphaera* involved in enhanced biological
636 phosphorus removal. *ISME J* 2013; **7**: 543–554.

637 67. Oyserman BO, Noguera DR, del Rio TG, Tringe SG, McMahon KD. Metatranscriptomic
638 insights on gene expression and regulatory controls in Candidatus Accumulibacter
639 phosphatis. *ISME J* 2016; **10**: 810–822.

640 68. Oehmen A, Lemos PC, Carvalho G, Yuan Z, Keller J, Blackall LL, et al. Advances in

enhanced biological phosphorus removal: From micro to macro scale. *Water Res* 2007; **41**: 2271–2300.

69. Comeau Y, Hall KJ, Hancock REW, Oldham WK. Biochemical Model for Enhanced Biological Phosphorus Removal. *Water Res* 1986; **20**: 1511–1521.

70. Mino T, Arun V, Tsuzuki Y, Matsuo T. Effect of phosphorus accumulation on acetate metabolism in the biological phosphorus removal process. *Biol. Phosphate Remov. from Wastewaters*. 1987. Pergamon, pp 27–38.

71. Hesselmann RPX, Von Rummell R, Resnick SM, Hany R, Zehnder AJB. Anaerobic Metabolism of Bacteria Performing Enhanced Biological Phosphate Removal. *Water Res* 2000; **34**: 3487–3494.

72. He S, McMahon KD. '*Candidatus* Accumulibacter' gene expression in response to dynamic EBPR conditions. *ISME J* 2011; **5**: 329–340.

73. Burow LC, Mabbett AN, Blackall LL. Anaerobic glyoxylate cycle activity during simultaneous utilization of glycogen and acetate in uncultured Accumulibacter enriched in enhanced biological phosphorus removal communities. *ISME J* 2008; **2**: 1040–1051.

74. Pramanik J, Trelstad PL, Schuler AJ, Jenkins D, Keasling JD. Development and validation of a flux-based stoichiometric model for enhanced biological phosphorus removal metabolism. *Water Res* 1999; **33**: 462–476.

75. Silva LG da, Gamez KO, Gomes JC, Akkermans K, Welles L, Abbas B, et al. Revealing metabolic flexibility of Candidatus Accumulibacter phosphatis through redox cofactor analysis and metabolic network modeling. *bioRxiv* 2018; 458331.

662 76. Rubio-Rincón FJ, Welles L, Lopez-Vazquez CM, Abbas B, van Loosdrecht MCM,
663 Brdjanovic D. Effect of Lactate on the Microbial Community and Process Performance of
664 an EBPR System. *Front Microbiol* 2019; **10**: 1–11.

665 77. Gao H, Mao Y, Zhao X, Liu W-T, Zhang T, Wells G. Genome-centric metagenomics
666 resolves microbial diversity and prevalent truncated denitrification pathways in a
667 denitrifying PAO-enriched bioprocess. *Water Res* 2019; **155**: 275–287.

668 78. Moreno-Vivián C, Cabello P, Martinez-Luque M, Blasco R, Castillo F. Prokaryotic
669 Nitrate Reduction□: Molecular Properties and Functional Distinction among Bacterial
670 Nitrate Reductases. *J Bacteriol* 1999; **181**: 6573–6584.

671 79. Siddiqui RA, Warnecke-Eberz U, Hengsberger A, Schneider B, Kostka S, Friedrich B.
672 Structure and function of a periplasmic nitrate reductase in Alcaligenes eutrophus H16. *J*
673 *Bacteriol* 1993; **175**: 5867–5876.

674 80. Richardson DJ, King GF, Kelly DJ, McEwan AG, Ferguson SJ, Jackson JB. The role of
675 auxiliary oxidants in maintaining redox balance during phototrophic growth of
676 *Rhodobacter capsulatus* on propionate or butyrate. *Arch Microbiol* 1988; **150**: 131–137.

677 81. Smith CB, Tolar BB, Hollibaugh JT, King GM. Alkane hydroxylase gene (alkB)
678 phylotype composition and diversity in northern Gulf of Mexico bacterioplankton. *Front*
679 *Microbiol* 2013; **4**: 370.

680 82. Wu B, Lan T, Lu D, Liu Z. Ecological and enzymatic responses to petroleum
681 contaminations. *Environ Sci Process Impacts* 2013; **16**: 1501–1509.

682 83. Welles L, Tian WD, Saad S, Abbas B, Lopez-Vazquez CM, Hooijmans CM, et al.

683 Accumulibacter clades Type I and II performing kinetically different glycogen-
684 accumulating organisms metabolisms for anaerobic substrate uptake. *Water Res* 2015; **83**:
685 354–366.

686

Figure Legends

Figure 1: Comparison of most abundant OTUs classified as *Ca*. Accumulibacter in Conventional A2O and S2EBPR SSRC configurations.

Figure 2: (A) Relative abundance of oligotypes of 16S rRNA gene amplicon sequences classified as *Ca.* Accumulibacter in conventional A2O and S2EBPR SSRC configurations (B) Phylogenetic tree of near full-length 16S rRNA gene sequences, that are exact matches to oligotypes, derived from metagenomic sequences using EMIRGE (highlighted in bold) and reference 16S rRNA gene sequences from He et al., (2007). Clade assignments for reference sequences are according to He et al., (2007) which were based on congruency with *ppk1* phylogeny (C) Relative Abundance of *ppk1* gene sequences extracted from the individual treatment-train assemblies and assigned clade-classification using pplacer.

Figure 3: (A)Phylogeny of Ca. Accumulibcter MAGs recovered from this study along with published draft genomes (n=19) of Accumulibacter, *Propionivibrio* and *Dechloromonas aromatica* as an outgroup based on a concatenated alignment of 37 marker genes. Genome bins recovered in this study are in bold. (B) *ppk1* genes from Ca. Accumulibacter genomes recovered from this study placed on a backbone reference tree created with 1012 sequences and classified according to He et al.,[21] (C) Relative abundance of MAGs recovered in this study.

Figure 4: Inventory of pathways in Accumulibacter MAGs associated with EBPR metabolism and denitrification. Blue and grey rectangles represent presence and absence of pathways based on annotation using KEGG.

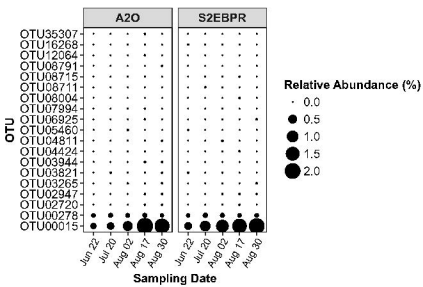
A2O
S2EBPR
OTU35307
OTU16268
OTU12064
OTU08791
OTU08715
OTU08711
OTU08004
OTU07994
OTU06925
OTU05460
OTU04811
OTU04424
OTU03944
OTU03821
OTU03265
OTU02947
OTU02720
OTU00278
OTU00015
OTU
Jun 22
Jul 20
Aug 02
Aug 17
Aug 30
Sampling Date
Relative Abundance (%)
0.0
0.5
1.0
1.5
2.0

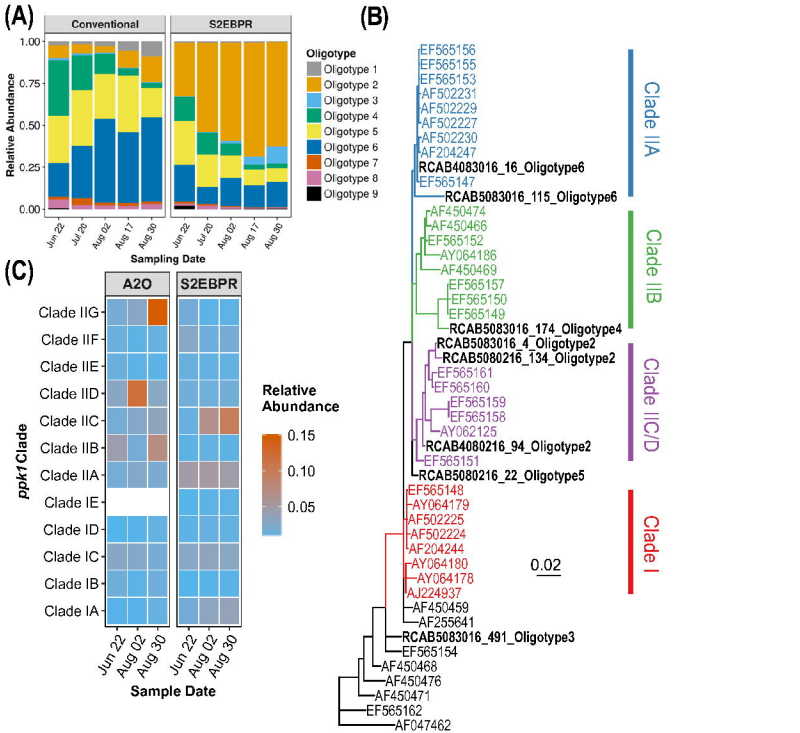
(A)
Conventional
S2EBPR
Relative Abundance
1.00
0.75
0.50
0.25
0.00
Jun 22
Jul 26
Aug 02
Aug 17
Aug 30
Sampling Date
Oligotype
Oligotype 1
Oligotype 2
Oligotype 3
Oligotype 4
Oligotype 5
Oligotype 6
Oligotype 7
Oligotype 8
Oligotype 9
(B)
EF565156
EF565155
EF565153
AF502231
AF502229
AF502227
AF502230
AF204247
RCAB4083016_16_Oligotype6
EF565147
RCAB5083016_115_Oligotype6
AF450474
AF450466
EF565152
AY064186
AF450469
EF565157
EF565150
EF565149
RCAB5083016_174_Oligotype4
RCAB5083016_4_Oligotype2
RCAB5080216_134_Oligotype2
EF565161
EF565160
EF565159
EF565158
AY062125
RCAB4080216_94_Oligotype2
EF565151
RCAB5080216_22_Oligotype5
EF565148
AY064179
AF502225
AF502224
AF204244
AY064180
AY064178
AJ224937
AF450459
AF255641
RCAB5083016_491_Oligotype3
EF565154
AF450468
AF450476
AF450471
EF565162
AF047462
0.02
Clade IIA
Clade IIB
Clade IIC/D
Clade I
(C)
A2O
S2EBPR
ppk1 Clade
Clade IIG
Clade IIF
Clade IIE
Clade IID
Clade IIC
Clade IIB
Clade IIA
Clade IE
Clade ID
Clade IC
Clade IB
Clade IA
Jun 22
Aug 02
Aug 30
Sample Date
Relative Abundance
0.15
0.10
0.05

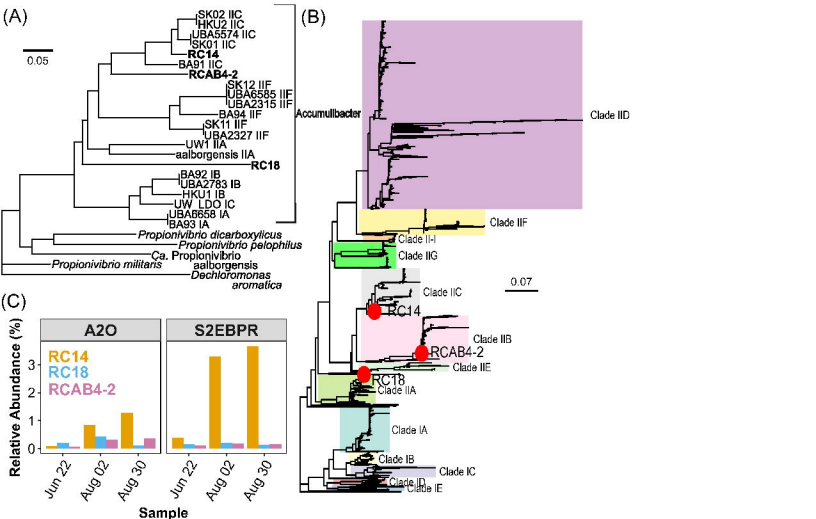
(A)
0.05
SK02 IIC
HK02 IIC
UBA5574 IIC
SK01 IIC
RC14
BA91 IIC
RCAB4-2
SK12 IIF
UBA6585 IIF
UBA2315 IIF
BA94 IIF
SK11 IIF
UBA2327 IIF
UW1 IIA
aalborgensis IIA
RC18
BA92 IB
UBA2783 IB
HKU1 IB
UW_LDO IC
UBA8658 IA
BA93 IA
Propionivibrio dicarboxylicus
Propionivibrio pelophilus
Ca. Propionivibrio aalborgensis
Propionivibrio militaris
Dechloromonas aromatica
(B)
Accumulibacter
Clade IID
Clade IIF
Clade II-I
Clade IIG
Clade IIC
0.07
RC14
Clade IIB
RCAB4-2
Clade IIE
RC18
Clade IIA
Clade IA
Clade IB
Clade IC
Clade ID
Clade IE
(C)
A2O
S2EBPR
RC14
RC18
RCAB4-2
Relative Abundance (%)
0
1
2
3
Jun 22
Aug 02
Aug 30
Sample

BA93
UBA6658
BA92
HKU1
UBA2783
UW-LDO-IC
RC18
aalborgensis
UW1
RCAB4-2
BA91
HKU2
RC14
SK01
SK02
UBA5574
BA94
SK11
SK12
UBA2315
UBA2327
UBA6585
Clade
IA
IB
IC
II
IIA
IIB
IIC
IIF
Cytochrome c-oxidation-cbb3
Cytochrome c-oxidation-aa3
High-affinity phosphate transport (PST)
Low-affinity phosphate transport (PiT)
PolyP Metabolism
TCA Cycle
EMP Pathway
PHA Metabolism
ED Pathway
Split TCA Cycle
Glyoxylate Shunt
Acetate Metabolism
Propionate Metabolism
Nitrate/Nitrite Transport
Respiratory Nitrate Reduction
Periplasmic Nitrate Reduction
Nitrite Reduction
Nitric Oxide Reduction
Nitrous Oxide Reduction